Journal of Clinical and Translational Hepatology **2023** vol. 11(1) | 110–117
DOI: 10.14218/JCTH.2021.00414

Original Article

Integrin α6 Targeted Near Infrared Fluorescent Imaging and Photoacoustic Imaging of Hepatocellular Carcinoma in Mice

Yan-Zhu Lin[1#], You Wu[1#], De-Hai Cao[1], Yong-Jian Peng[1], Jun Deng[2], Wen-Jie Lin[1], Min-Yi Si-Tu[1], Ling Zhuo[1], Jie-Min Chen[1], Man-Xia Lei[3], Rong-Bin Liu[4], Wei-Guang Zhang[1], Jian-Jun Li[1], Xiao-Chun Yang[1*] and Guo-Kai Feng[1*]

[1]State Key Laboratory of Oncology in South China, Collaborative Innovation Center for Cancer Medicine, Sun Yat-sen University Cancer Center, Guangzhou, Guangdong, China; [2]Guangdong Institute for Drug Control, Department of Biologic Products, Guangzhou, Guangdong, China; [3]Department of Endocrinology, Nanfang Hospital, Southern Medical University, Guangzhou, Guangdong, China; [4]Department of Ultrasound, Sun Yat-sen Memorial Hospital, Sun Yat-sen University, Guangzhou, Guangdong, China

Received: 15 September 2021 | **Revised:** 15 February 2022 | **Accepted:** 17 March 2022 | **Published:** 12 April 2022

Abstract

Background and Aims: Hepatocellular carcinoma (HCC) is the fourth most common cause of cancer-related death and ranks sixth in terms of incident cases worldwide. The purpose of this study was to develop an effective and sensitive method to distinguish liver cancer tissues from normal tissues in HCC patients. Integrin α6 is a promising cell surface target for molecular imaging of HCC, where it is overexpressed and is a prognostic biomarker. We previously identified an integrin α6-targeted peptide CRWYDENAC (RWY) that has been used for positron emission tomography (PET) imaging of HCC in mouse models. ***Methods:*** We labeled the integrin α6-targeted RWY peptide with cyanine 7 (Cy7) to form an optical probe (Cy7-RWY) for near infrared fluorescent (NIRF) and photoacoustic (PA) imaging in HCC. Mice transplanted with subcutaneous HCC-LM3 or orthotopic HCC-H22 cells that overexpressed integrin α6 were intravenously injected with Cy7-RWY and its corresponding Cy7-control. NIRF and PA images of mice were collected from 0 to 48 h after injection. ***Results:*** Both NIRF and PA signals started to accumulate in the tumor 2 h after injection of Cy7-RWY and peaked at 24 h. ***Conclusions:*** Cy7-RWY is a promising optical probe for NIRF and PA imaging of HCC in mice, and has potential clinical application for HCC detection.

Citation of this article: Lin YZ, Wu Y, Cao DH, Peng YJ, Deng J, Lin WJ, *et al*. Integrin α6 Targeted Near Infrared Fluorescent Imaging and Photoacoustic Imaging of Hepatocellular Carcinoma in Mice. J Clin Transl Hepatol 2023; 11(1):110–117. doi: 10.14218/JCTH.2021.00414.

Keywords: Photoacoustic imaging; Near-infrared fluorescent imaging; Integrin α6; Peptide; Molecular imaging; Hepatocellular carcinoma.

Abbreviations: HCC, hepatocellular carcinoma; PET, positron emission tomography; Cy7, cyanine 7; NIRF, near infrared fluorescent; PA, photoacoustic; MR, magnetic resonance; PBS, phosphate buffered saline; ROI, region of interest.

[#]Contributed equally to this work.

[*]**Correspondence to:** Guo-Kai Feng and Xiao-Chun Yang, Sun Yat-sen University Cancer Center/Cancer Hospital, State Key Laboratory of Oncology in South China, 651 Dongfeng East Road, Guangzhou, Guangdong 510060, China. ORCID: https://orcid.org/0000-0002-8251-291X (GKF), https://orcid.org/0000-0002-5508-5000 (XCY). Tel: +86-20-87340256 (GKF) +86-13503048769 (XCY), E-mail: mailto:fengguok@sysucc.org.cn (GKF), mailto:yangxch@sysucc.org.cn (XCY)

Introduction

Hepatocellular carcinoma (HCC) accounts for the majority of primary liver cancers. Worldwide, liver cancers are the fourth most common cause of cancer-related death and rank sixth in incident cases. According to GLOBOCAN 2018, the incidence of liver cancer is increasing, with an estimated 841,000 new cases and 782,000 deaths worldwide. Because of the absence of early symptoms and limitations of conventional imaging modalities for detection, the majority of HCC patients are diagnosed at an unresectable advanced stage with an extremely poor prognosis.[1,2] Therefore, more effective methods for HCC detection are urgently required.

Targeted molecular imaging with high specificity and sensitivity is an attractive technique for HCC detection that has achieved promising results in animal models in recent studies.[3–6] Near infrared fluorescent (NIRF) imaging (650–900 nm) is a noninvasive approach with high sensitivity and specific imaging ability. It is widely used in basic science, medical research, and drug development. However, poor spatial resolution and insufficient depth penetration limit its application.[7] Photoacoustic (PA) imaging is a novel noninvasive imaging modality combining the advantages of optical and acoustic imaging. It generates three-dimensional images that provide excellent spatial resolution in living organisms.[8,9] Photoacoustic imaging (PAI) uses either endogenous signals like hemoglobin or an exogenous targeted contrast agent that is typically used for molecular imaging. The potential application of PA imaging in cancers has attracted intensive research interest.[10,11] In recent years, a series of side-viewing PA imaging systems have been developed and validated on small animal models, including *in situ* gastric cancer detection, melanoma in rat colorectum *in vivo*, and HCC xenograft tumors *in vivo*.[12]

Integrin α6, is an adhesion molecule located on the cell surface, and it is involved in cell attachment and multiple aspects of cancer invasion and metastasis.[13] Many studies provide evidence that the integrin α6 is overexpressed in HCC

patients with particularly poor survival, and that it appears to have a significant role in tumor progression.[14–17] We previously reported that integrin α6 overexpression occurs in approximately 94% of clinical early-stage HCCs and in mice is overexpressed in subcutaneous HCC-LM3 tumors compared with liver tissue.[18] Several pathways have also been found to be involved in the function of integrin α6 in HCC development, such as the MAPK/ERK[19] and PI3K/AKT[15] signaling pathways. The evidence suggests that integrin α6 is a potential target for molecular imaging in HCC detection. Among the molecular-targeted imaging probes, peptides have advantages of small size, low toxicity, highly efficient clearance from nontarget tissues, and deep penetration into tissue, which are of great interest.[20] Some of the peptides that have been investigated and successfully used for tumor receptor imaging and cancer detection/targeted therapeutics are Arg-Gly-Asp (RGD),[21] ^{111}In-DTPA-octreotide,[22] and anti-Her2/neu peptide (AHNP).[23]

We previously identified a tumor-targeted peptide CRWYDENAC (RWY) by phage display technology and confirmed that it binds to integrin a6 with high specificity and affinity and can be used for nasopharyngeal carcinoma-specific nanotherapeutics.[24] Recently, we translated this integrin a6-targeted peptide into a positron emission tomography (PET) probe, ^{18}F-RWY, and explored its application for PET imaging of HCC in four different mouse HCC models.[18] We also successfully constructed RWY peptide as an MR contrast agent, RWY-dL-(Gd-DOTA)4, for magnetic resonance (MR) imaging of HCC.[25] In addition, our optimized integrin a6-targeted MR probe, DOTA(Gd)-ANADYWR, efficiently visualized small HCC lesions.[26] RWY peptide has been used as a molecular probe in other carcinomas, such as pancreatic,[27] colorectal, and breast cancer.[29] We demonstrated the feasibility of this targeted peptide for the detection of HCC patients in future clinical applications. In this study, we labeled RWY peptide with cyanine 5 (Cy5) to form an optical probe (Cy5-RWY) that specifically homed to HCC lesions in orthotopic HCC mice (Supplementary Fig. 1). However, the Cy5 wavelength is not suitable for PA imaging. We then labeled RWY peptide with cyanine 7 (Cy7) to form an optical probe (Cy7-RWY) that may be suitable for PA imaging. The characteristics, biodistribution, and imaging performance of this novel probe for PA imaging of HCC cancer were evaluated *in vitro* and *in vivo*. The results supported the potential application of Cy7-RWY for HCC detection by PA imaging.

Methods

Peptide synthesis

The integrin a6-targeted fluorescent peptides (Cy7-RWY and Cy5-RWY) were synthesized by solid-phase chemistry and were purchased from the Chinese Peptide/Protein Core facility. The peptide imaging agent includes nine amino acids (Cys-Arg-Trp-Tyr-Asp-Glu-Asn-Ala-Cys) and cyclized by the formation of a disulfide bonds. The negative control peptide (Cys-Gly-Gly-Gly-Gly-Gly-Gly-Gly-Cys) was previously described by Sugahara *et al*.[30]

Cell culture and animal models

Mouse hepatocellular carcinoma cell lines H22 and Hepa1-6 and human hepatocellular carcinoma cell lines LM3, PLC/PRF/5, HepG2, and Huh7 were purchased from the American Type Culture Collection (Manassas, VA, USA). Cells were cultivated in Dulbecco's modified Eagle's medium (Life Technologies, Grand Island, NY, USA) containing 10% fetal bovine serum and 1% pen/strep (100 U/mL penicillin and 100 U/mL streptomycin) and incubated at 37°C and 5% CO_2.

Balb/c nude mice (18±2 g, 4 weeks of age) were obtained from the Animal Center of Vital River, Charles River China (Beijing, China). To obtain orthotopic transplantation tumor models, 1×10^6 of luciferase-tagged HCC-LM3 cells in 50% Matrigel (BD Biosciences, San Jose, CA) were injected into the left lateral lobe of the liver. For subcutaneous transplantation tumor models, 4×10^6 of HCC-LM3 or HCC-H22 cells were administered by subcutaneous injection in the right flank of mice. The growth of liver cancer was monitored by bioluminescence imaging.[31,32]

Cytotoxicity assay

The *in vitro* cytotoxicity of Cy7-RWY peptide was determined by cell counting Kit-8 assay (CCK-8). Briefly, H22 cells were seeded in 96-well plates at a density of 3×10^3 cells in 100 μL of medium per well. After 24 h, cells were incubated with concentrations of Cy7-RWY peptide ranging from 0 to 500 nM for 48 h or 72 h. For assay, 10 μL of CCK-8 solution (Dojindo, Kumamoto, Japan) was added to each well, and the cells were incubated for an additional 2 h. Absorption was measured at 450 nm by a TECAN Infinite M1000PRO microplate reader (TECAN, Victoria, Austria).

In vitro cellular uptake

For confocal fluorescence microscopy, HCC-LM3 cells were seeded on 24-well glass coverslips. After 24 h of attachment, cells were incubated with Cy7-RWY (6 nM) for 2 h, washed with phosphate buffered saline (PBS) three times, and fixed with 4% paraformaldehyde for 10 m. The cells were permeabilized with 0.2% Triton X-100/PBS for 20 m, blocked with 5% bovine serum albumen, and incubated with primary antibodies against integrin a6 (dilution 1:250; Cell Signaling Technology) overnight at 4°C. Slides were then washed and incubated with fluorescein-conjugated goat anti-rabbit secondary antibodies (dilution 1:1,000; Cell Signaling Technology) for 1 h at 37°C. Nuclei were stained with diamidino-phenylindole and observed with a confocal microscope (Olympus FV1000, Tokyo, Japan). For cellular uptake of Cy7-RWY, cells were incubated with 10 μg Cy7-RWY dissolved in 500 μL PBS at 4°C for 20 m with stirring, washed with PBS three times, and unbound Cy7-RWY was removed by centrifugation. Cellular fluorescence was read by flow cytometry (Beckman-Coulter).

NIR fluorescence imaging

HCC-LM3 tumor-bearing mice were intravenously injected with 10 nM Cy7-RWY in 100 μL 0.9% saline. NIR fluorescence imaging was performed at various times after injection with an IVIS Imaging Spectrum System and IVIS 4.2 Living Imaging software (Perkin Elmer; Waltham, MA, USA).

PA imaging

PA imaging was performed with an Endra Nexus 128 PA tomography system (Endra, Michigan, USA) that provides wavelengths from 680 to 900 nm. The PA signals of Cy7-RWY at different concentrations were determined with a laser pulse of 750 nm. During image acquisition, a bowl-like tray with a dimple in the center was used for immobilizing the imaging positions in the center and filled with 1 mL water. Nude mice with subcutaneous HCC-LM3 tumors were placed in a water bath and anesthetized by intraperitoneal

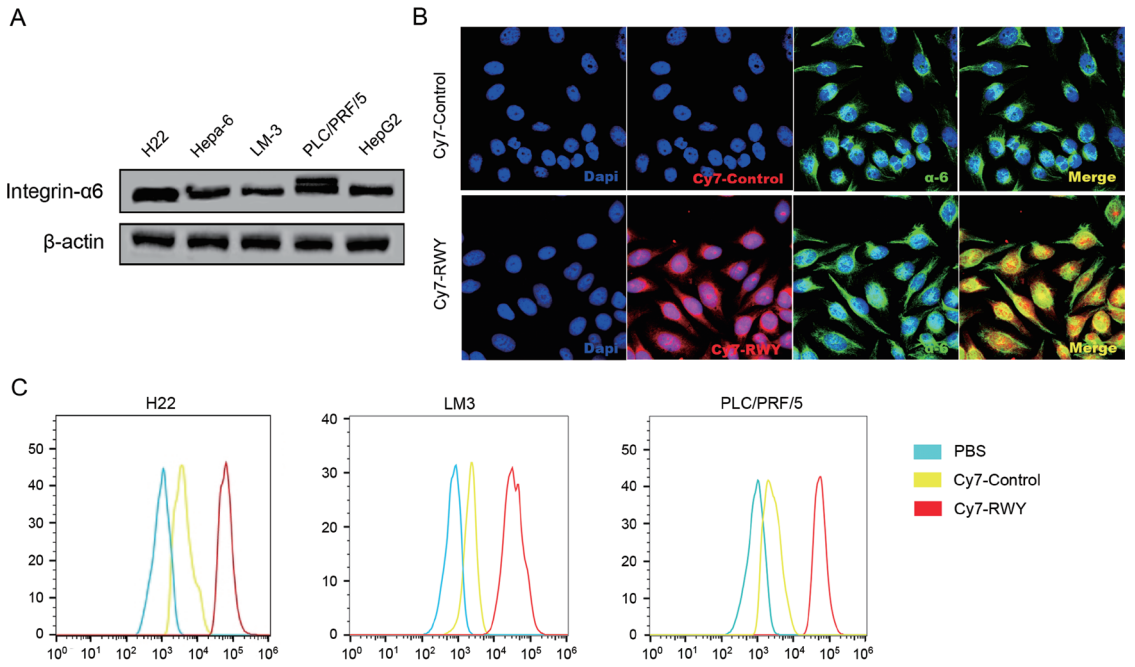

Fig. 1. Integrin α6-target probe Cy7-RWY binds to HCC cells. (A) The expression of integrin α6 in the HCC cell lines. (B) Colocalization of Cy7-RWY peptide and integrin α6 in HCC-LM3 cells imaged by confocal microscope. (C) Flow cytometry assay of the binding affinity of Cy7-RWY to HCC cells. HCC, hepatocellular carcinoma.

injection of pentobarbital sodium (40 mg/kg). Cy7-RWY was intravenously injected into the tail vein (20 nM, 150 μL in PBS). PA imaging at 750 and 800 nm was performed before injection and at various times after injection. For *ex vivo* PA imaging, mice were sacrificed and the harvested organs were immediately placed in the PA imaging system.

RWY biodistribution

Tumor-bearing mice were sacrificed 48 h after injection of Cy7-RWY. The tissues were homogenized in PBS buffer and the homogenate was passed through 40 μm cell strainers to obtain clear tissue solutions. The distribution of RWY in the various organs was measured by Cy7 fluorescence and flow cytometry. The imaging studies were performed when the tumor volumes were about 100 mm^3. The NIRF images of mice were obtained with the *in vivo* imaging system, a 740 nm excitation wavelength and a 780 nm filter. Immediately after imaging, the mice were sacrificed and heart, liver, spleen, kidney, lung, brain, and tumor were harvested for *ex vivo* imaging as described above.

Bioluminescence imaging

Bioluminescence imaging of luciferase-tagged HCC-LM3 cells or tumors was performed with a Xenogen IVIS Spectrum Imaging System and analyzed with Living Image software (PerkinElmer) by measurement of photon flux in the tumor region of interest in mice. Data were normalized to the background signal.

Immunohistochemistry

After sacrifice, the major organs were fixed in 4% formaldehyde, embedded in paraffin, sectioned, and stained with hematoxylin and eosin. After blocking nonspecific antigens with 5% fetal bovine serum, sections were incubated overnight at 4°C with a primary antibody against integrin α6 (Abcam, USA). After washing with PBS Tween three times, sections were incubated with a secondary antibody for 1 h at room temperature and observed with a digital microscope (Leica QWin).

Statistical analysis

PA signal intensity was measured by region of interest (ROI) analysis with IVIS 4.2 Living Imaging software and the results were reported as means±SD. The statistical calculations were performed with GraphPad Prism v.5 (GraphPad Software, Inc.; San Diego, CA, USA) and $p < 0.05$ was considered to be statistically significant.

Results

Binding of Cy7-RWY peptide to HCC cells

The expression of integrin a6 in HCC cell lines was evaluated by western blotting. As shown in Figure 1A, integrin a6 was highly expressed in HCC cell lines. Fluorophore Cy7 was used to label the N-terminus of RWY peptide to form an imaging probe (Cy7-RWY, Supplementary Fig. 2). The binding affinity of Cy7-RWY was confirmed by confocal microscopy using HCC-LM3 cells. Strong red fluorescence signals of the Cy7-RWY were observed in HCC-LM3 cells, whereas the Cy7-control without targeting, showed no fluorescence response (Fig. 1B). Flow cytometry analysis was further performed to investigate the binding ability of Cy7-RWY. Cy7-RWY peptides displayed significantly higher cellular uptake than nontargeted peptides (Fig. 1C). Cytotoxicity of Cy7-RWY was evaluated by CCK-8. As shown in Supplementary

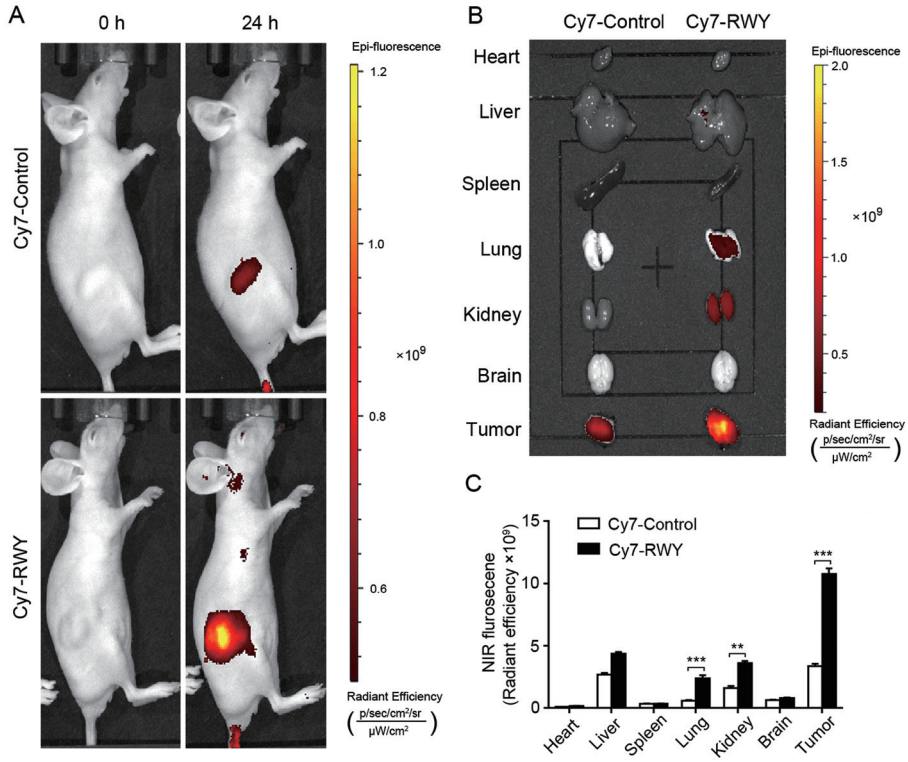

Fig. 2. NIRF imaging with Cy7-RWY in subcutaneous HCC-LM3 tumor-bearing mice. (A) *In vivo* fluorescence images of mice before (0 h) and at 24 h after tail-vein intravenous injection of Cy7-RWY. (B) *Ex vivo* NIRF images of major organs and tumor 24 h post-injection. (C) Quantitative analysis of NIRF signal intensity in major organs and tumors 24 h post-injection. Student's *t*-test, $n=3$, $^{**}p<0.01$; $^{***}p<0.001$. NIRF, near infrared fluorescent.

Figure 3, no significant cytotoxicity was observed in H22 cells at increasing concentrations of Cy7-RWY, indicating the biocompatibility of the peptide. The results showed that Cy7-RWY had a high binding affinity to HCC cells *in vitro*.

Biodistribution and tumor-targeting ability of Cy7-RWY

NIRF imaging was performed to evaluate the tumor-targeting ability of Cy7-RWY *in vivo* using a subcutaneous HCC-LM3 tumor model. Figure 2A shows NIRF imaging of tumors before and after injection of Cy7-RWY. A strong fluorescence signal intensity was observed in the tumor site but little accumulation of fluorescence signals was observed in in the Cy7-control group. In an *ex vivo* analysis, the mice were sacrificed 24 h post-injection for harvesting and imaging of tumor tissue and organs (heart, lung, liver, spleen, kidneys and brain) for IVIS Lumina XR system quantitative biodistribution analysis. The biodistribution of Cy7-RWY and Cy7-control in the corresponding mice groups was evaluated by drawing ROI along the excised tumors and organs. As shown in Figure 2B, consistent with the *in vivo* observation, a strong signal was exhibited by tumors treated with Cy7-RWY peptide, indicating selective targeted of the tumor site. Quantitative analysis of the accumulation of dye intensity in organs is shown in Figure 2C. These results show that Cy7-RWY effectively and specifically accumulated in tumors.

In vivo fluorescence imaging of the HCC orthotopic transplantation tumor model carried out at various times showed that the fluorescence intensity reached the strongest level in orthotopic HCC-LM3 tumors at 24 h after systemic delivery (Supplementary Fig. 4). Figures 3 and Supplementary Figure 5 also show the localization of Cy7-RWY in orthotopic HCC-H22 tumors by *in vivo* fluorescence imaging. After the mice were sacrificed, *ex vivo* fluorescence images of tumor tissue and major organs from mice were obtained 48 h after injection. The high level of the fluorescence signal found in the tumors of the mice that received Cy7-RWY suggested effective accumulation of the peptide in the tumor at the time of observation. After the imaging procedures, we observed strong staining of integrin α6 of tumor sections by immunohistochemistry (Supplementary Fig. 6). Confocal examination of tumor sections found significant colocalization of Cy7-RWY (red fluorescence) and integrin α6 receptor in HCCs from mice (Supplementary Fig. 7), which confirmed highly efficient tumor targeting by Cy7-RWY. Major organs were harvested to analyze the biodistribution of Cy7-RWY. Flow cytometry revealed that, compared with the control group, liver cancer lesions had significantly higher fluorescence signals (Supplementary Fig. 8). We evaluated the *in vivo* toxicity of the imaging dose of Cy7-RWY. H&E staining did not find significant cell and tissue damage in major organs including the heart, spleen, lung, kidney and brain compared with the control group (Supplementary Fig. 9). We further assessed the biosafety of Cy7-RWY peptide in excess dose in normal mice and mice bearing subcutaneous HCC-LM3 tumors by routine blood examination (Supplementary Fig. 10) and H&E staining of the heart, liver, spleen, lung, and kidney (Supplementary Fig. 11). The results provided strong evidence of the high tumor-targeting efficiency of the Cy7-RWY peptide.

Photoacoustic properties of Cy7-RWY peptide

Cy7-RWY was used as an integrin a6 tracker for PAI *in vivo*

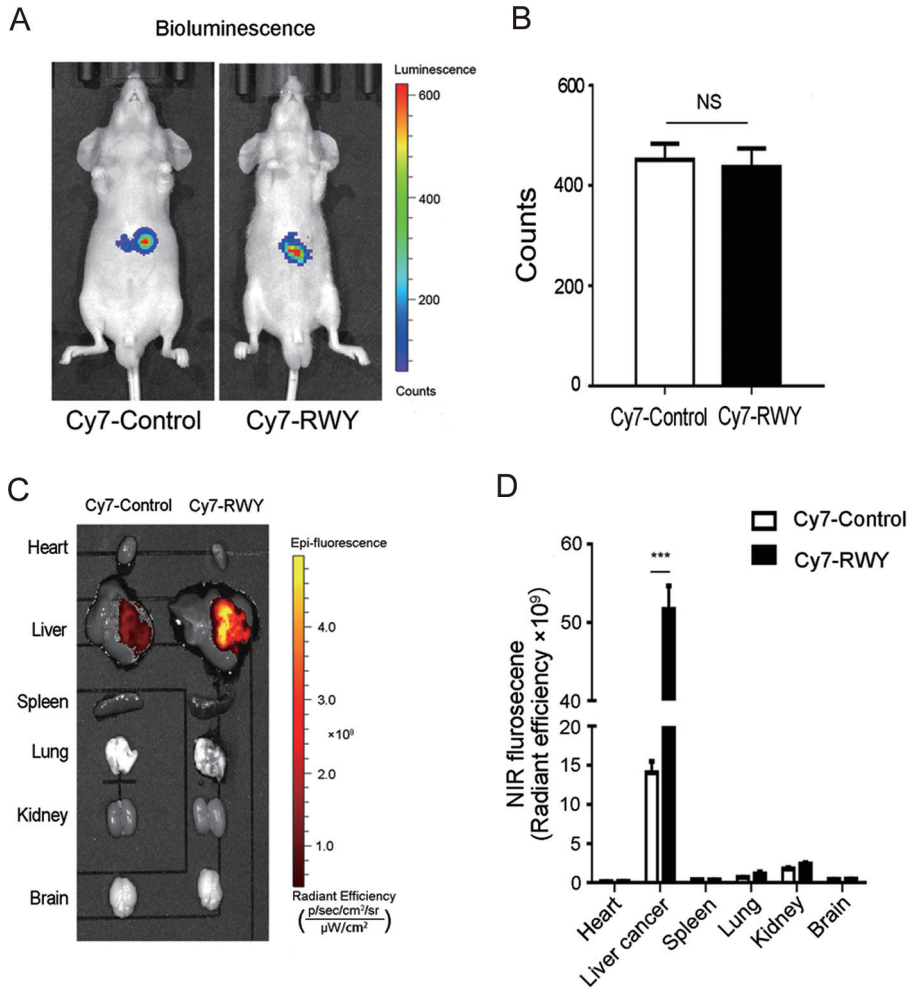

Fig. 3. NIRF imaging with Cy7-Control and Cy7-RWY in orthotopic HCC-H22 tumor-bearing mice. (A) The luminescence imaging signals were observed in the hepatic regions. (B) Quantification of luminescence imaging signals in the hepatic regions. (C) *Ex vivo* fluorescence images of major organs and tumors at 48 h post-injection. (D) Quantification of fluorescence intensity extracted from the organs. Student's *t*-test, $n=3$, $^{***}p<0.001$. NIRF, near infrared fluorescent

as shown in Figure 4A. For evaluation, tumor-bearing mice were anesthetized and placed in the center of a tray. In the UV-vis spectrum, with increasing excitation, Cy7-RWY yielded a characteristic peak at 744 nm at a concentration of 100 nM (Fig. 4B). Photoacoustic signals at different concentrations of Cy7-RWY increased as the Cy7-RWY concentration increased (Fig. 4C), and the fluorescence intensity of Cy7-RWY was positively correlated with Cy7 concentration (Fig. 4D). The results support the use of Cy7-RWY as a probe for biological applications.

Photoacoustic imaging with Cy7-RWY in mice with subcutaneous HCC

We performed *in vivo* PA imaging in mice bearing subcutaneous HCC-LM3 cells at various times. Mice were intravenously injected with Cy7-RWY, followed by PAI before injection), and at 1, 2, 4, 6, and 24 h after injection. The photoacoustic signal was calculated by drawing an ROI around the tumor. As shown in Figure 5A, before injection only large blood vessels in the tumor could be visualized using hemoglobin as an endogenous contrast agent (at 750 nm and 800 nm). One hour after intravenous injection of Cy7-RWY, we found consistently increasing photoacoustic signals, indicating that Cy7-RWY passively targeted tumor tissues in a short period of time. The PA signals reached maximum accumulation at 24 h for Cy7-RWY (Fig. 5A), indicating prolonged circulation time in the bloodstream. Imaging of tumor blood vessels was possible with an endogenous hemoglobin agent at 800 nm. Photoacoustic signals were observed in the important metabolic organs, such as the liver and kidney (Fig. 5B). Quantitative analyses of photoacoustic signal enhancement in the tumor regions at different times after injection (Fig. 5C) provided substantial evidence for the tumor-targeting ability of Cy7-RWY.

Discussion

Previously, we used phage display technology to identify a tumor-targeted peptide RWY, and confirmed its target as integrin α6.[24] In this study, we developed an integrin α6-targeted NIRF and PA imaging agent, Cy7-RWY and focused on its use in HCC. We confirmed that integrin α6 was expressed at a relatively high level in all HCC cell lines, and that the RWY peptide specifically bound to HCC cells *in vitro*. The integrin α6-overexpressing HCC cells HCC-LM3 and HCC-H22 were used to establish subcutaneous and ortho-

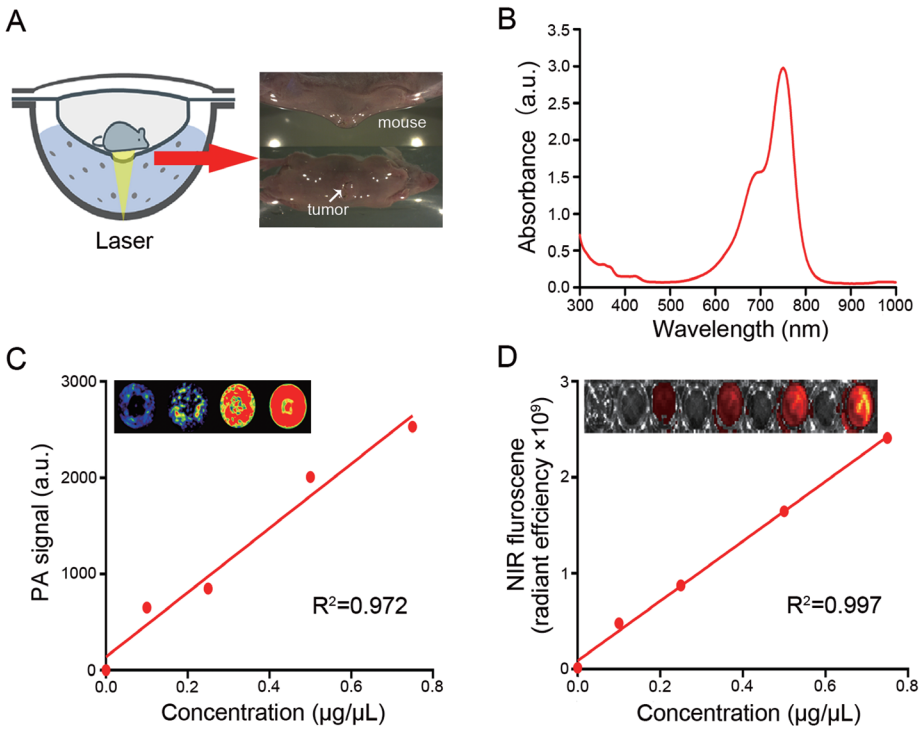

Fig. 4. Characteristics of the Cy7-RWY peptide. (A) Schematic of the photoacoustic imaging system. (B) UV-vis-NIR spectra of Cy7-RWY peptide. (C) PA signals with different concentrations of Cy7-RWY at 760 nm and the linear relationship between PA signal intensity and the different concentrations of Cy7-RWY. (D) The near infrared fluorescence signal of the Cy7-RWY. PA, photoacoustic.

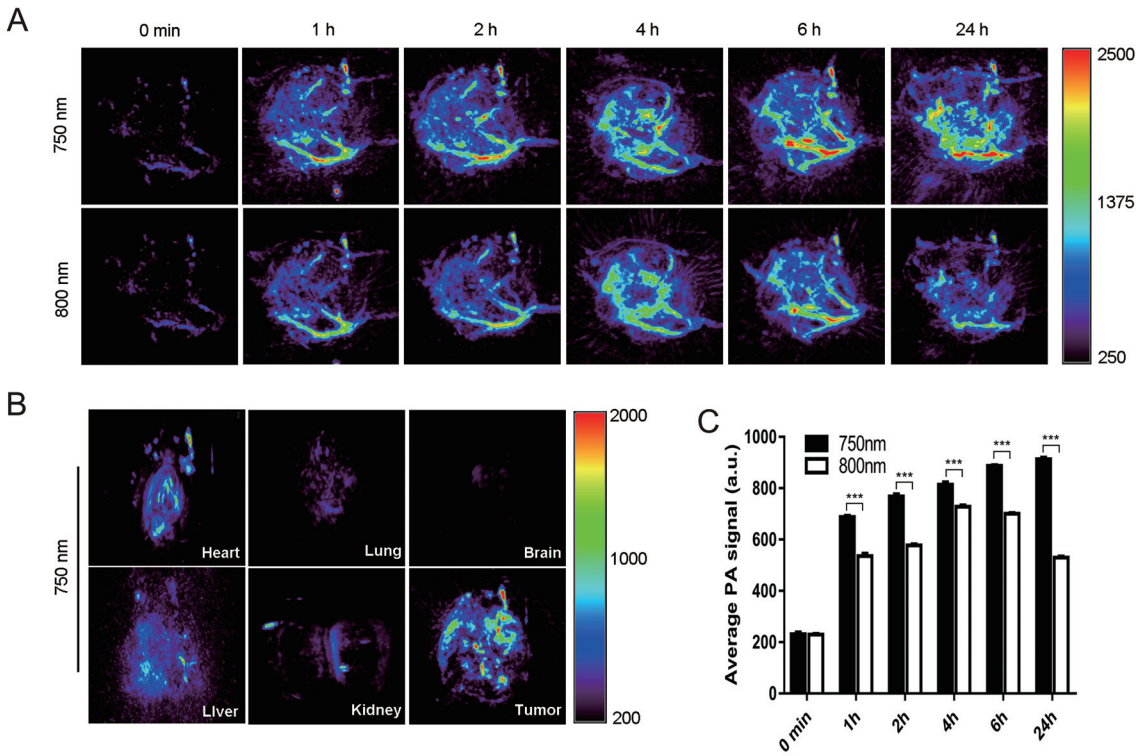

Fig. 5. Photoacoustic imaging in mice bearing subcutaneous HCC-LM3 tumors. (A) *In vivo* PA imaging of the tumor areas before (0 min) and 1, 2, 4, 6, and 24 h after injection of Cy7-RWY. (B) *Ex vivo* quantification of PA signals of major organs and tumors from mice 24 h post-injection. (C) Quantitative analyses of PA signals of tumor tissues *in vivo*. Student's *t*-test, $n=3$, ***$p<0.001$. PA, photoacoustic.

tropic HCC tumors in mice. *In vivo* PA/NIRF imaging showed Cy7-RWY effectively and specifically accumulated in HCC tumors. The data indicate that Cy7-RWY has potential as an agent for PA imaging of α6-overexpressing HCCs.

Cell targeting peptides are a class of targeting moieties used as delivery vehicles for HCC diagnosis and imaging.[20] Recent advances in developing different targeted peptides provide exciting new possibilities for targeted therapy in HCC. Using mass spectrometry, Lee *et al*.[33] identified L5 (Thr-Tyr-Phe-Leu-Thr-Arg-Gln) peptide targeting glypican-3 expressing HCC cells, which supports its use as suitable homing moiety for HCC diagnosis and targeted therapy. Du *et al*.[34] showed that the peptide A54 screened from the phage display library was a novel targeting therapy vector in doxorubicin delivery for HCC target therapy. In addition, LO *et al*.[35] demonstrated that the conjugation of SP94 and liposomal doxorubicin enhanced the therapeutic efficacy against HCC xenografts.

Molecular imaging is an emerging diagnostic approach for oncology applications. Recently, interest in peptides as probes for dual-modality tumor imaging there has increased. Chen *et al*. described the use of plectin-1 targeted nanoparticles for fluorescence/MR dual-modal imaging in pancreatic cancer.[36] Dual-modality (MRI/SPECT) molecular imaging was shown to be a powerful diagnostic tool for the early diagnosis of mesothelin-expressing cancers.[37] The results of this study showed that the novel optical probe, Cy7-RWY peptide, bound specifically to integrin α6 in HCC *in vitro* and *in vivo*. Cy7, an NIR fluorophore with longer wavelength absorption and emission provides deeper tissue penetration to achieve good signal and should be a strong contrast agent for NIRF and PA imaging. Therefore, optical imaging with the Cy7 labeling method has great potential for the highly sensitive and accurate visualization of tumor microfoci that overexpress integrin α6. In this study, we found that integrin α6 was expressed at a relatively high level in HCC cell lines. Colocalization of Cy7-RWY and integrin a6 was observed in HCC cells, and fluorescence activated cell sorting supported the results. The *in vivo* integrin a6 binding specificity was confirmed biodistribution and imaging studies. In both subcutaneous and orthotopic HCC tumor xenografts, the results demonstrated the presence of NIRF signals localized exclusively in the HCC-LM3 or HCC-H22 tumor model in a time-dependent manner with relatively low uptake by nontargeted organs. However, spatial resolution is the major limitation of the technique. Therefore, mice bearing subcutaneous HCC-LM3 tumors were given Cy7-RWY through vein tail to allow systemic circulation and were subjected to photoacoustic radiation at different times. Before injection, there was only a weak PA signal detected in the tumor tissue. After injection, enhanced PA signals were visible in tumor tissue, and they increased gradually with time, indicating good tumor accumulation of Cy7-RWY after systemic administration. Compared with NIRF imaging, PA had significantly higher spatial resolution. The PA signal in the tumor was very strong at 24 h, suggesting high tumor-targeting efficiency. In our study, the fluorescence signal reached a steady level already after 6 h and was sustained until 24 h post-injection, thus providing a broad clinically useful time window for imaging. Imaging agent toxicity is a concern for which there is relatively little data. The Cy7-RWY probe showed no toxicity in major organs including the heart, lung, liver, spleen, and kidney, and had fast renal clearance. Given the data, Cy7-RWY provided extremely high sensitivity for the detection of liver tumor foci. Studies of intraoperative resection, drug carriers, therapy monitoring, and cancer diagnosis will benefit from Cy7-RWY peptide guided imaging.

There are several limitations in our study. Firstly, although the PA signal has good tissue penetration, systemic imaging is rarely done because of the limited scanning range of the machine. It is challenging to use for whole-body imaging as applied in diagnostic systems and intraoperative imaging for clinical applications. Secondly, it is difficult for the targeted Cy7-RWY peptide to detect early HCC lesions with a small diameter without optimization. Thirdly, we did not determine whether Cy7-RWY peptide is suitable for malignant metastatic HCC. We are now exploring the feasibility of our peptide in differentiating tumors from abnormal liver tissues such as fibrosis, and from regenerative nodules.

Conclusions

In summary, we successfully constructed an integrin α6-targeted probe, Cy7-RWY with promising biocompatibility and good optical stability. It is suitable for NIRF and PA imaging of HCC. Upon further development and validation, the Cy7-RWY probe may contribute to the accurate delineation of liver tumor foci and may have wide clinical application in early diagnosis and accurate surgical excision in the future.

Funding

This study was funded by the National Natural Science Foundation of China (Grant: 81972531), Fundamental Research Funds for the Central Universities (Grant: 19ykpy174), GuangDong Basic and Applied Basic Research Foundation (Grant: 2020A1515011374) and GuangDong Basic and Applied Basic Research Foundation (Grant: 202102020138).

Conflict of interest

The authors have no conflict of interests related to this publication.

Author contributions

Performance of experiments, collection of data, analysis of results, and writing of the manuscript (YZL, YW, XCY, DHC), provision of technological and associated help (YJP, JD, WJL, MYT, LZ, JMC, MXL, RBL, WGZ), design and supervision of experiments, and modification of the manuscript (JJL and GKF).

Ethical statement

All animal experiment procedures were approved by the Experimental Animal Welfare and Ethical Committee of Sun Yat-Sen University Cancer Center and were performed following the guidelines for the care and use of laboratory animals of Sun Yat-sen University Cancer Center.

Data sharing statement

No additional data are available.

References

[1] Glantzounis GK, Paliouras A, Stylianidi MC, Milionis H, Tzimas P, Roukos D, *et al*. The role of liver resection in the management of intermediate and advanced stage hepatocellular carcinoma. A systematic review. Eur J Surg Oncol 2018;44(2):195–208. doi:10.1016/j.ejso.2017.11.022, PMID:2925

8719.
[2] Villanueva A. Hepatocellular Carcinoma. N Engl J Med 2019;380(15):1450–1462. doi:10.1056/NEJMra1713263, PMID:30970190.
[3] Yasui Y, Kurosaki M, Izumi N. [Imaging diagnosis and molecular profiling of hepatocellular carcinoma]. Nihon Shokakibyo Gakkai Zasshi 2016;113(5):785–789. doi:10.11405/nisshoshi.113.785, PMID:27151474.
[4] Song J, Zhang F, Ji J, Chen M, Li Q, Weng Q, *et al*. Orthotopic hepatocellular carcinoma: molecular imaging-monitored intratumoral hyperthermia-enhanced direct oncolytic virotherapy. Int J Hyperthermia 2019;36(1):344–350. doi:10.1080/02656736.2019.1569731, PMID:30776922.
[5] Li G, Chi CW, Shao XF, Fang CH. Application of molecular imaging technology in evaluating the inhibiting effect of apigenin in vivo on subcutaneous hepatocellular carcinoma. Biochem Biophys Res Commun 2017;487(1):122–127. doi:10.1016/j.bbrc.2017.04.029, PMID:28408212.
[6] Gharib AM, Thomasson D, Li KC. Molecular imaging of hepatocellular carcinoma. Gastroenterology 2004;127(Suppl 1):(5):S153–158. doi:10.1053/j.gastro.2004.09.029, PMID:15508079.
[7] Petrovsky A, Schellenberger E, Josephson L, Weissleder R, Bogdanov A Jr. Near-infrared fluorescent imaging of tumor apoptosis. Cancer Res 2003;63(8):1936–1942. PMID:12702586.
[8] Bam R, Laffey M, Nottberg K, Lown PS, Hackel BJ, Wilson KE. Affibody-Indocyanine Green Based Contrast Agent for Photoacoustic and Fluorescence Molecular Imaging of B7-H3 Expression in Breast Cancer. Bioconjug Chem 2019;30(6):1677–1689. doi:10.1021/acs.bioconjchem.9b00239, PMID:31082216.
[9] Wang LV, Hu S. Photoacoustic tomography: in vivo imaging from organelles to organs. Science 2012;335(6075):1458–1462. doi:10.1126/science.1216210, PMID:22442475.
[10] Witte RS, Tamimi EA. Emerging photoacoustic and thermoacoustic imaging technologies for detecting primary and metastatic cancer and guiding therapy. Clin Exp Metastasis 2022;39(1):213–217. doi:10.1007/s10585-021-10095-x, PMID:33950414.
[11] Zhao Z, Swartchick CB, Chan J. Targeted contrast agents and activatable probes for photoacoustic imaging of cancer. Chem Soc Rev 2022;51(3):829–868. doi:10.1039/d0cs00771d, PMID:35094040.
[12] Du J, Yang S, Qiao Y, Lu H, Dong H. Recent progress in near-infrared photoacoustic imaging. Biosens Bioelectron 2021;191:113478. doi:10.1016/j.bios.2021.113478, PMID:34246125.
[13] Bon G, Folgiero V, Di Carlo S, Sacchi A, Falcioni R. Involvement of alpha-6beta4 integrin in the mechanisms that regulate breast cancer progression. Breast Cancer Res 2007;9(1):203. doi:10.1186/bcr1651, PMID:17319974.
[14] Bergamini C, Sgarra C, Trerotoli P, Lupo L, Azzariti A, Antonaci S, *et al*. Laminin-5 stimulates hepatocellular carcinoma growth through a different function of alpha6beta4 and alpha3beta1 integrins. Hepatology 2007;46(6):1801–1809. doi:10.1002/hep.21936, PMID:17948258.
[15] Ke AW, Shi GM, Zhou J, Huang XY, Shi YH, Ding ZB, *et al*. CD151 amplifies signaling by integrin α6β1 to PI3K and induces the epithelial-mesenchymal transition in HCC cells. Gastroenterology 2011;140(5):1629–1641.e1615. doi:10.1053/j.gastro.2011.02.008, PMID:21320503.
[16] Begum NA, Mori M, Matsumata T, Takenaka K, Sugimachi K, Barnard GF. Differential display and integrin alpha 6 messenger RNA overexpression in hepatocellular carcinoma. Hepatology 1995;22(5):1447–1455. doi:10.1002/hep.1840220518, PMID:7590662.
[17] Liu LX, Jiang HC, Liu ZH, Zhou J, Zhang WH, Zhu AL, *et al*. Integrin gene expression profiles of human hepatocellular carcinoma. World J Gastroenterol 2002;8(4):631–637. doi:10.3748/wjg.v8.i4.631, PMID:12174369.
[18] Feng GK, Ye JC, Zhang WG, Mei Y, Zhou C, Xiao YT, *et al*. Integrin α6 targeted positron emission tomography imaging of hepatocellular carcinoma in mouse models. J Control Release 2019;310:11–21. doi:10.1016/j.jconrel.2019.08.003, PMID:31400382.
[19] Weng CJ, Chau CF, Hsieh YS, Yang SF, Yen GC. Lucidenic acid inhibits PMA-induced invasion of human hepatoma cells through inactivating MAPK/ERK signal transduction pathway and reducing binding activities of NF-kappaB and AP-1. Carcinogenesis 2008;29(1):147–156. doi:10.1093/carcin/bgm261, PMID:18024477.
[20] Araste F, Abnous K, Hashemi M, Taghdisi SM, Ramezani M, Alibolandi M. Peptide-based targeted therapeutics: Focus on cancer treatment. J Control Release 2018;292:141–162. doi:10.1016/j.jconrel.2018.11.004, PMID:30408554.
[21] Chen X, Hou Y, Tohme M, Park R, Khankaldyyan V, Gonzales-Gomez I, *et al*. Pegylated Arg-Gly-Asp peptide: 64Cu labeling and PET imaging of brain tumor alphavbeta3-integrin expression. J Nucl Med 2004;45(10):1776–1783. PMID:15471848.
[22] Lee S, Xie J, Chen X. Peptide-based probes for targeted molecular imaging. Biochemistry 2010;49(7):1364–1376. doi:10.1021/bi901135x, PMID:20102226.
[23] Park BW, Zhang HT, Wu C, Berezov A, Zhang X, Dua R, *et al*. Rationally designed anti-HER2/neu peptide mimetic disables P185HER2/neu tyrosine kinases in vitro and in vivo. Nat Biotechnol 2000;18(2):194–198. doi:10.1038/72651, PMID:10657127.
[24] Feng GK, Zhang MQ, Wang HX, Cai J, Chen SP, Wang Q, *et al*. Identification of an Integrin α6-Targeted Peptide for Nasopharyngeal Carcinoma-Specific Nanotherapeutics. Advanced Therapeutics 2019;2(7):1900018. doi:10.1002/adtp.201900018.
[25] Zhang Y, Zhao J, Cai J, Ye JC, Xiao YT, Mei Y, *et al*. Integrin α6-Targeted Magnetic Resonance Imaging of Hepatocellular Carcinoma in Mice. Mol Imaging Biol 2020;22(4):864–872. doi:10.1007/s11307-019-01437-z, PMID:31792839.
[26] Lin BQ, Zhang WB, Zhao J, Zhou XH, Li YJ, Deng J, *et al*. An Optimized Integrin α6-Targeted Magnetic Resonance Probe for Molecular Imaging of Hepatocellular Carcinoma in Mice. J Hepatocell Carcinoma 2021;8:645–656. doi:10.2147/jhc.S312921.
[27] Mei Y, Li YH, Yang XC, Zhou C, Li ZJ, Zheng XB, *et al*. An optimized integrin alpha6-targeted peptide for positron emission tomography/magnetic resonance imaging of pancreatic cancer and its precancerous lesion. Clin Transl Med 2020;10(4):e157. doi:10.1002/ctm2.157, PMID:32898323.
[28] Xiao YT, Zhou C, Ye JC, Yang XC, Li ZJ, Zheng XB, *et al*. Integrin alpha6-Targeted Positron Emission Tomography Imaging of Colorectal Cancer. ACS Omega 2019;4(13):15560–15566. doi:10.1021/acsomega.9b01920, PMID:31572857.
[29] Gao S, Jia B, Feng G, Dong C, Du H, Bai L, *et al*. First-in-human pilot study of an integrin alpha6-targeted radiotracer for SPECT imaging of breast cancer. Signal Transduct Target Ther 2020;5(1):147. doi:10.1038/s41392-020-00266-9, PMID:32782265.
[30] Sugahara KN, Teesalu T, Karmali PP, Kotamraju VR, Agemy L, Girard OM, *et al*. Tissue-penetrating delivery of compounds and nanoparticles into tumors. Cancer Cell 2009;16(6):510–520. doi:10.1016/j.ccr.2009.10.013, PMID:19962669.
[31] Liu M, Zheng S, Zhang X, Guo H, Shi X, Kang X, *et al*. Cerenkov luminescence imaging on evaluation of early response to chemotherapy of drug-resistant gastric cancer. Nanomedicine 2018;14(1):205–213. doi:10.1016/j.nano.2017.10.001, PMID:29045825.
[32] Zhang Z, Cai M, Bao C, Hu Z, Tian J. Endoscopic Cerenkov luminescence imaging and image-guided tumor resection on hepatocellular carcinoma-bearing mouse models. Nanomedicine 2019;17:62–70. doi:10.1016/j.nano.2018.12.017, PMID:30654183.
[33] Lee YL, Ahn BC, Lee Y, Lee SW, Cho JY, Lee J. Targeting of hepatocellular carcinoma with glypican-3-targeting peptide ligand. J Pept Sci 2011;17(11):763–769. doi:10.1002/psc.1400, PMID:21976137.
[34] Du B, Han H, Wang Z, Kuang L, Wang L, Yu L, *et al*. targeted drug delivery to hepatocarcinoma in vivo by phage-displayed specific binding peptide. Mol Cancer Res 2010;8(2):135–144. doi:10.1158/1541-7786.Mcr-09-0339, PMID:20145035.
[35] Lo A, Lin CT, Wu HC. Hepatocellular carcinoma cell-specific peptide ligand for targeted drug delivery. Mol Cancer Ther 2008;7(3):579–589. doi:10.1158/1535-7163.Mct-07-2359, PMID:18347144.
[36] Chen X, Zhou H, Li X, Duan N, Hu S, Liu Y, *et al*. Plectin-1 Targeted Dual-modality Nanoparticles for Pancreatic Cancer Imaging. EBioMedicine 2018;30:129–137. doi:10.1016/j.ebiom.2018.03.008, PMID:29574092.
[37] Misri R, Meier D, Yung AC, Kozlowski P, Hafeli UO. Development and evaluation of a dual-modality (MRI/SPECT) molecular imaging bioprobe. Nanomedicine 2012;8(6):1007–1016. doi:10.1016/j.nano.2011.10.013, PMID:22100757.